

### Supporting Information

## **An ESIPT based versatile fluorescent probe for bioimaging strong acidic conditions in Live-cells and *E. coli***

Nancy Singla<sup>a</sup>, Manzoor Ahmad<sup>a</sup>, Sukhvinder Dhiman<sup>a</sup>, Gulshan Kumar<sup>b</sup>, Siloni Singh<sup>c</sup>, Shagun Verma<sup>c</sup>, Satwinderjeet Kaur<sup>c</sup>, Muzamil Rashid<sup>d</sup>, Sukhraj Kaur<sup>d</sup>, Vijay Luxami<sup>b</sup>, Prabhpreet Singh<sup>a</sup> and Subodh Kumar<sup>\*a</sup>

- <sup>a.</sup> Department of Chemistry, Center for Advanced Studies, Guru Nanak Dev University, Amritsar - 143005  
<sup>b.</sup> School of Chemistry and Biochemistry, Thapar Institute of Engineering and Technology, Patiala-147004  
<sup>c.</sup> Department of Botanical and Environment Science, Guru Nanak Dev University, Amritsar 143005  
<sup>d.</sup> Department of Microbiology, Guru Nanak Dev University, Amritsar 143005

Figure S1: <sup>1</sup> H NMR spectrum of compound 3	Page 2
Figure S2: <sup>13</sup> C NMR spectrum of compound 3	Page 2
Figure S3: HRMS of compound 3	Page 3
Figure S4: <sup>1</sup> H NMR spectrum of probe <b>BTNN</b>	Page 3
Figure S5: <sup>13</sup> C NMR spectrum of probe <b>BTNN</b>	Page 4
Figure S6: HRMS of probe <b>BTNN</b>	Page 4
Experimental general and procedures	Page 5-7
Figure S7: Effect of pH on the absorption spectrum of <b>BTNN</b>	Page 8
Figure S8: The fluorescence spectra of <b>BTNN</b> in the presence of metal ions and H <sup>+</sup>	Page 8
Figure S9: (A) The fluorescence spectra of <b>BTNN</b> in water – glycerol binary mixtures; (B) plot of fluorescence intensity of <b>BTNN</b> against increasing $f_{glycerol}$	Page 8
Figure S10: The photo stability of probe <b>BTNN</b>	Page 9
Figure S11: The optimized geometries of normal and keto forms of <b>BTNN</b>	Page 9
Figure S12: The comparison of energies of the <b>BTNN</b> obtained after protonation at diethylamino nitrogen, benzothiazole nitrogen and aldehyde oxygen	Page 9
Figure S13: The optimized structure of <b>BTNN</b> and <b>BTNNH</b>	Page 10
Figure S14: Fluorescence spectra of <b>BTNN</b> at pH 2 on excitation at 370 nm and at 430 nm	Page 10
Figure S15: The MTT experiments of <b>BTNN</b> under different concentrations for MG-63 cells	Page 10
Figure S16: Fluorescence images of the MG-63 cells stained with 10 μM <b>BTNN</b> at (A) pH 2.6 (B) pH 3.6 (C) pH 4.6.	Page 10
Table S1. Comparison of physical behaviour and applications of <b>BTNN</b> with reported fluorescent probes	Page 11-13

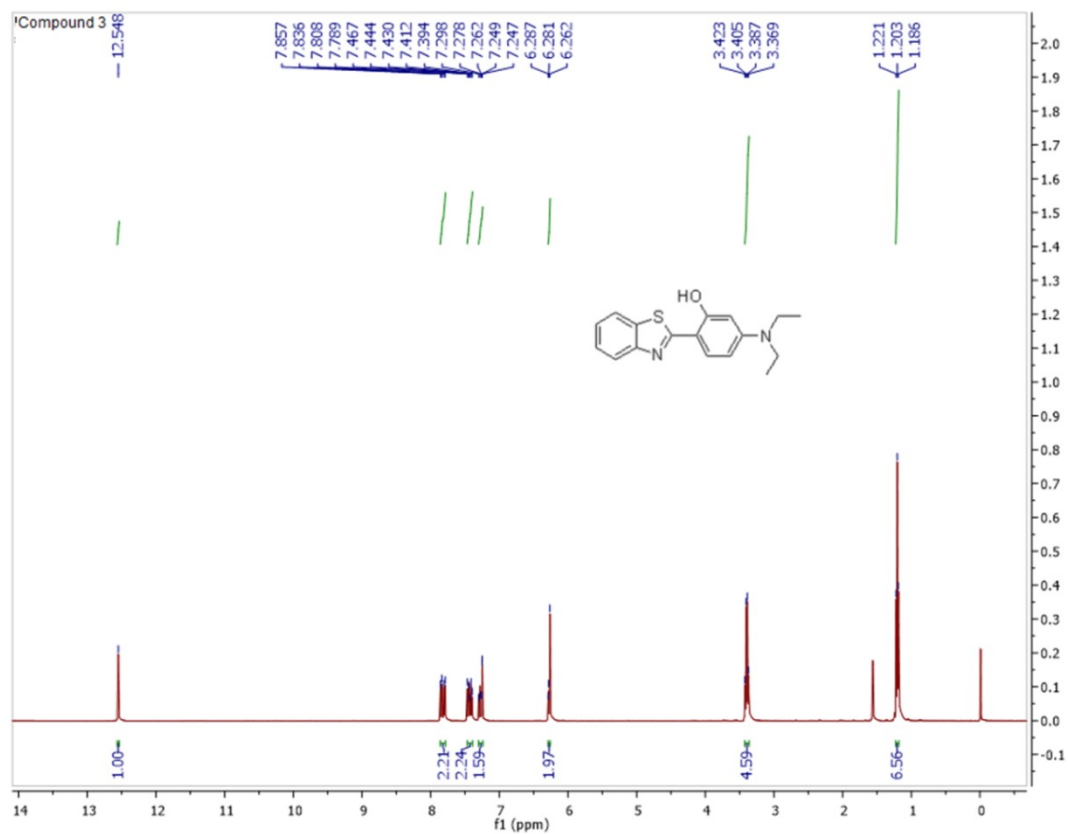


Figure S1:  $^1\text{H}$  NMR spectrum of compound 3

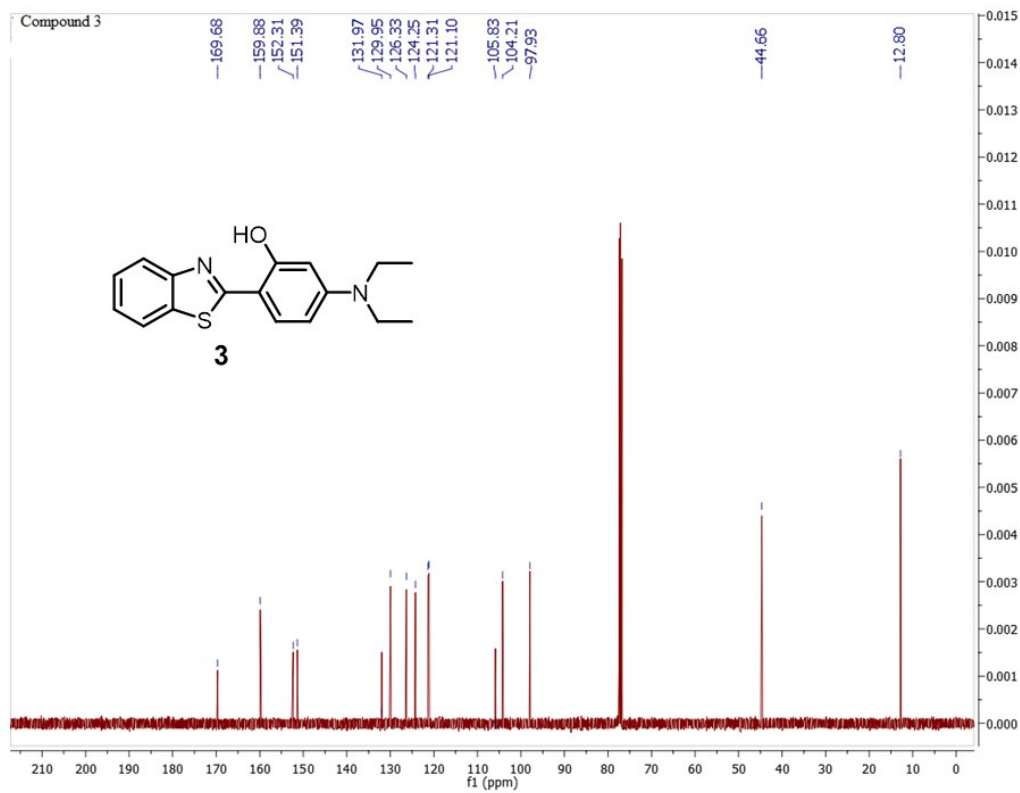


Figure S2:  $^{13}\text{C}$  NMR spectrum of compound 3

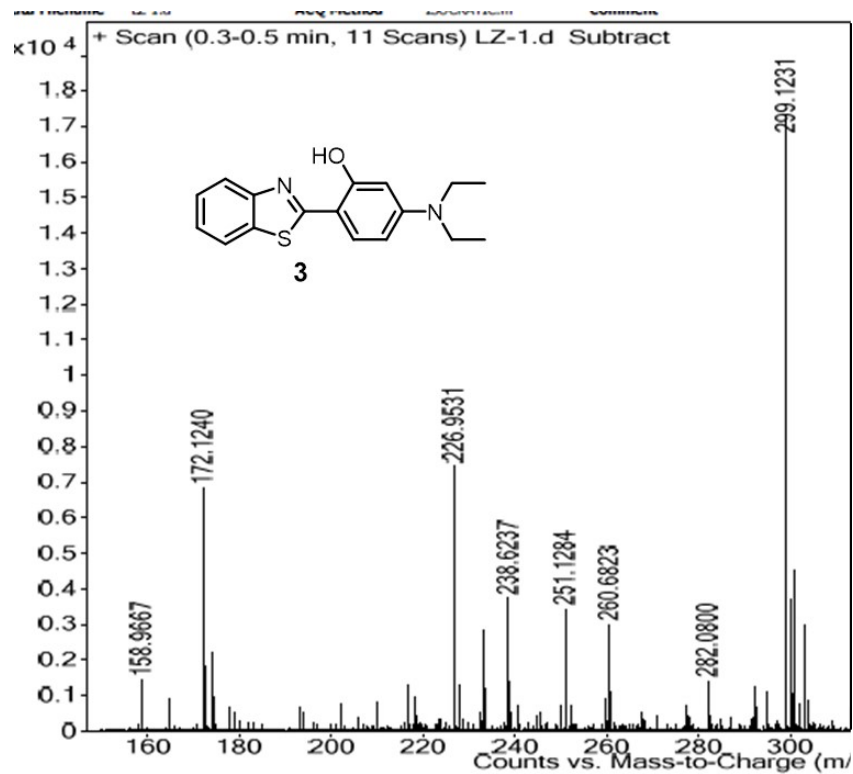


Figure S3: HRMS of compound 3

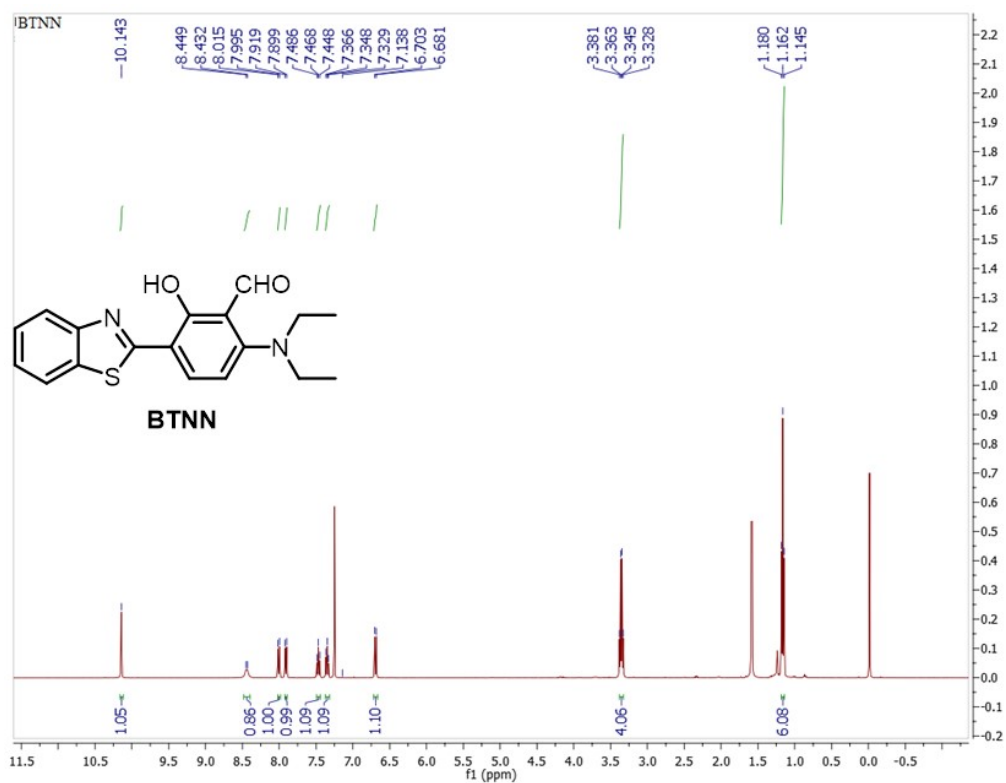


Figure S4: <sup>1</sup>H NMR spectrum of probe BTNN

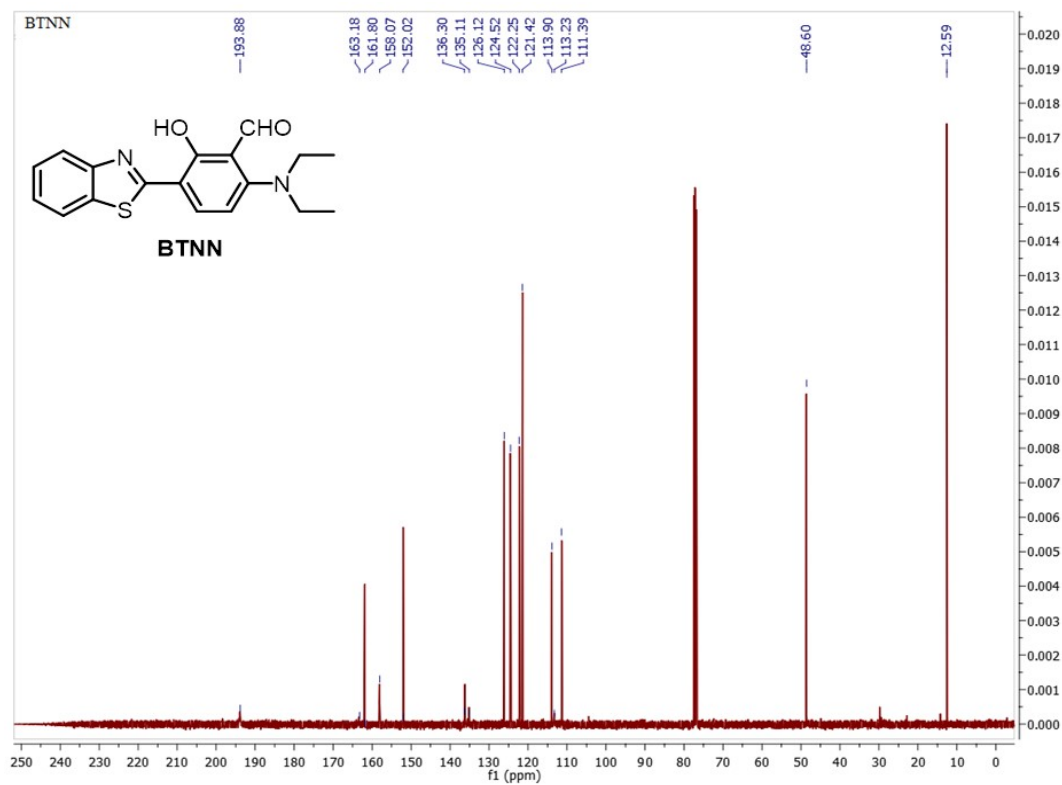


Figure S5: <sup>13</sup>C NMR spectrum of probe **BTNN**

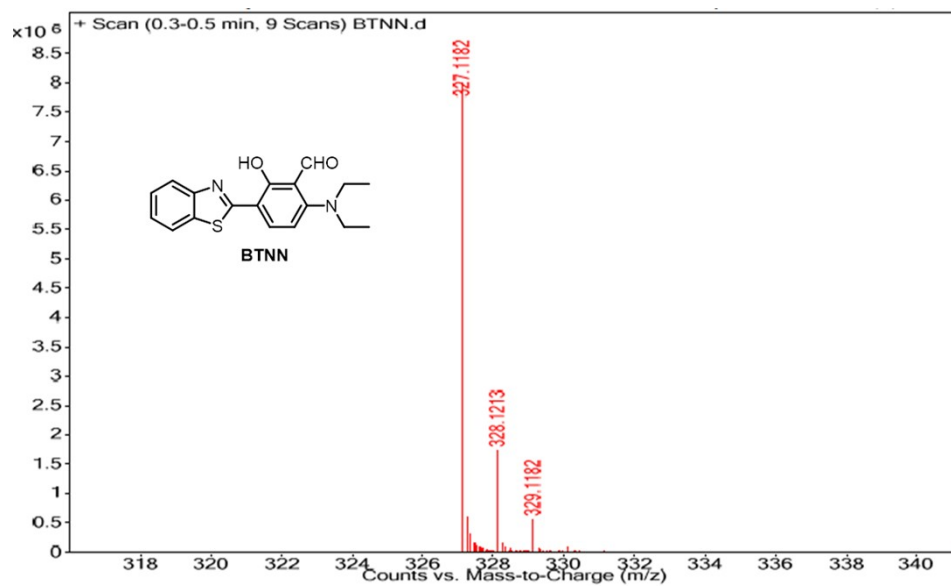


Figure S6: HRMS of probe **BTNN**

## Experimental general and procedures

Chemicals were purchased from Sigma and Spectrochem India, and were used as purchased. The solvent THF was distilled before use. JEOL 400 MHz FT NMR machine was used for recording  $^1\text{H}$  and  $^{13}\text{C}$  NMR spectra. The chemical shift and coupling constant (J) values of peaks in NMR are respectively in ppm (relative to TMS internal standard) and Hz. The multiplicity of signals is as s = singlet, d = doublet, t = triplet, q = quartet, m = multiplet. High resolution mass spectra were recorded on Agilent 6520 Q-TOF Mass Spectrometer with Agilent 1200 HPLC System at CDRI Lucknow. Ultra UV/UF Rions lab water system was used for having deionized water. The spectrophotometers Shimadzu UV-2450 and Horiba Fluorolog-3 were used to obtain absorbance and emission spectra.

## UV-Vis and Fluorescence Studies

The stock solution of the probe **BTNN** (1 mM) in THF was used for photophysical studies. For pH studies, 1.5 ml of stock solution was diluted to 150 ml using Millipore water to prepare 10  $\mu\text{M}$  solution of **BTNN**. The pH of this solution was determined using TIMPL pH meter (Ahmadabad). To evaluate the effect of pH on absorbance and emission properties of **BTNN**, their pH values were adjusted between pH 2-12 by using HCl and NaOH solutions and 10 ml of this solution were transferred to different volumetric flasks. For determining the effect of different amounts of water on absorption and fluorescence spectra of **BTNN**, 100  $\mu\text{l}$  of stock solution was poured in 10 ml volumetric flasks and these were diluted with different binary mixtures of THF and HEPES buffer (0.01 M, pH 7.2). Similarly for viscosity studies, the 100  $\mu\text{l}$  stock solution was diluted with binary mixtures of glycerol and HEPES buffer.

The UV-Vis and fluorescence spectra of all these solutions were recorded. All fluorescence and absorption data were saved as ASCII files and graphs were drawn using Microsoft Excel. The quantum yields of the solutions were calculated by Horiba Fluorolog-3 spectrophotometer using integrating sphere and optical band pass filter. In order to find the pKa value of **BTNN**, the entire spectral data of **BTNN** obtained at different pH values was evaluated using the software SPECFIT-32. The pKa values, the distribution of the species and their binding constants were determined through the fit model.

## MTT assay

Probe **BTNN** was investigated for its cytotoxic potential in MG-63 cells using MTT [3-(4,5-diethylthiazol-2-yl)-2,5-diphenyl tetrazolium bromide] assay. MG-63 cells were seeded in 96

well plate and incubated in CO<sub>2</sub> incubator (5%) for 24 h. The cells were treated with different concentrations of **BTNN** (5, 10, 25, 50 µM) for 24 h. Thereafter, 5µl of MTT dye (5 mg/ml) was added to each well and kept in CO<sub>2</sub> incubator for 2-4 h. The supernatant was decanted off followed by the addition of DMSO (100 µl) in each well. Finally, absorbance of the final solution was recorded at 570 nm using Synergy H1 Microplate reader, biotek.

### **Fluorescence imaging of pH in MG-63 (osteosarcoma) cells**

MG-63 (osteosarcoma) cells were cultured and maintained in Dulbecco's modified eagle medium (DMEM) supplemented with 10 % FBS (fetal bovine serum) and incubated at 37°C in CO<sub>2</sub> incubator (5%). MG-63 cells were seeded in 24 well plate with coverslips and incubated in CO<sub>2</sub> incubator (5%) for 24 hr. After confluency, DMEM medium was replaced with fresh Buffer solutions of different pH (2.6, 3.6, 4.6 and 7.6) (Citric Acid – Na<sub>2</sub>HPO<sub>4</sub> Buffer) with **BTNN** in each well and incubated in CO<sub>2</sub> incubator for 30 min. Thereafter, cells were washed thrice with 1× PBS buffer to remove excess **BTNN** in each well. Then, the coverslips were mounted onto the slides with the help of flouramount and cell imaging was performed on Nikon Eclipse Ts2 Fluorescent Microscope.

### **Fluorescence imaging of pH in *E. coli* bacteria**

Gram-negative bacterium *Escherichia coli* NCIM 5662 was procured from National Collection of Industrial Microorganisms (NCIM), Pune, India. For obtaining the culture of *E. coli*, single colony of the bacteria from the streaked Luria-Bertani (LB) agar plate was transferred to LB broth (tryptone 10 g/L, yeast extract 5 g/L, and NaCl 10 g/L) in a test tube and incubated overnight at 37°C under aerobic conditions. *E. coli* 5662 was cultured overnight and centrifuged at 10000 rpm for 3 min to obtain the bacterial pellet. The sediment was washed with sterile water and then was re-suspended in solutions (1000 µl) of different pH 2.6, 3.6, 4.6 and 7.6. The 5 µl solution of **BTNN** (1 mM, DMSO) was added to every tube to a final probe concentration of 5 µM. *E. coli* with the probe were incubated for 10 min. After 10 min, the suspensions were centrifuged at 10000 rpm for 3 min and the unbound **BTNN** supernatant was removed. The bacterial pellets were washed twice and re-suspended in PBS (pH 7.4). Thin smears of the bacterial suspensions were prepared on grease-free glass slides and the slides were observed under fluorescent Microscope (Nikon Eclipse Ts2) in blue channel.

### **<sup>1</sup>H NMR titration of BTNN with TFA**

The solution of **BTNN** (2 mM, CDCl<sub>3</sub>) was taken in NMR tube. The aliquots of 8.4 μL amounts of TFA were added gradually and <sup>1</sup>H NMR spectrum was recorded after each addition.

### **Detection of acid vapours by BTNN-polystyrene thin films**

To make the polystyrene thin films, 500 mg polystyrene was dissolved in CHCl<sub>3</sub> (10 mL) and 200 μL solution of **BTNN** (1 mM, CHCl<sub>3</sub>) was added to it. The solution was allowed to stand for 24 h. This solution (100 μL) was poured on a TLC glass slide and was spread over 2 cm length. The solvent was allowed to evaporate and respective film was stored at 25°C in thermostat. For vapour phase detection of HCl, **BTNN**-polystyrene films were placed in a 2800 cc box and 16 μL of 10 N HCl was dropped in the box. After 30 seconds, **BTNN**-polystyrene film was removed and was viewed under 365 nm UV lamp.

### **BTNN coated TLC strips**

TLC strips were dipped in solution of **BTNN** (10 μM, ethanol) for 2 min and were then allowed to dry in thermostat at 25°C for an hour. These TLC strips were treated with 10 μL of different concentrations of HCl and were viewed under 365 nm light.

### **Theoretical studies**

The geometries of **BTNN** and its protonated species **BTNNH** were optimized both at ground state (S<sub>0</sub>) and excited state (S<sub>1</sub>) using density functional theory (DFT) and time dependent DFT (TDDFT) methods. The geometrical optimization at S<sub>0</sub> were carried out using B3LYP / PBEPBE functional and 6-311g(d) basis set. Further, integral equation formalism polarizable continuum model (IEFPCM) was used for aqueous environment. The incorporation of 6-311+g(d,p), 6-311+g(d,p) and TZVP level basis set did not affect the results significantly and therefore, we continued with cost-effective 6-311g(d) basis set. Based on the optimized configurations, the geometrical parameters such as bond lengths and angles, frontier molecular orbitals, the relative energies of geometries, absorption and emission properties were calculated. The potential energy curves (PECs) at S<sub>0</sub> and S<sub>1</sub> states were constructed along the intramolecular hydrogen bonds. All the calculations were completed with Gaussian 16 B.01 program.

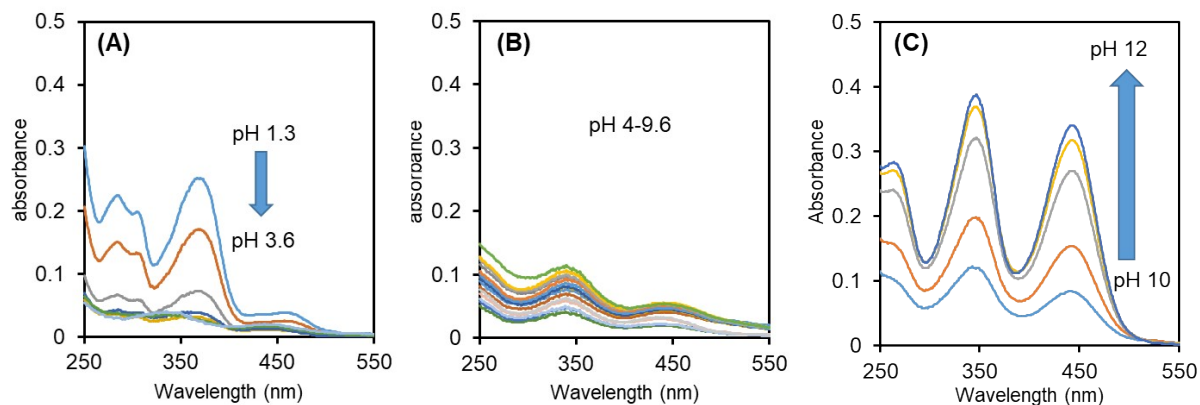


Figure S7: Effect of pH on the absorption spectrum of **BTNN**

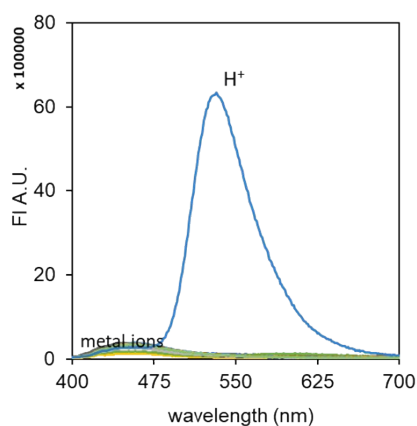


Figure S8: The fluorescence spectra of **BTNN** in the presence of metal ions and H<sup>+</sup>

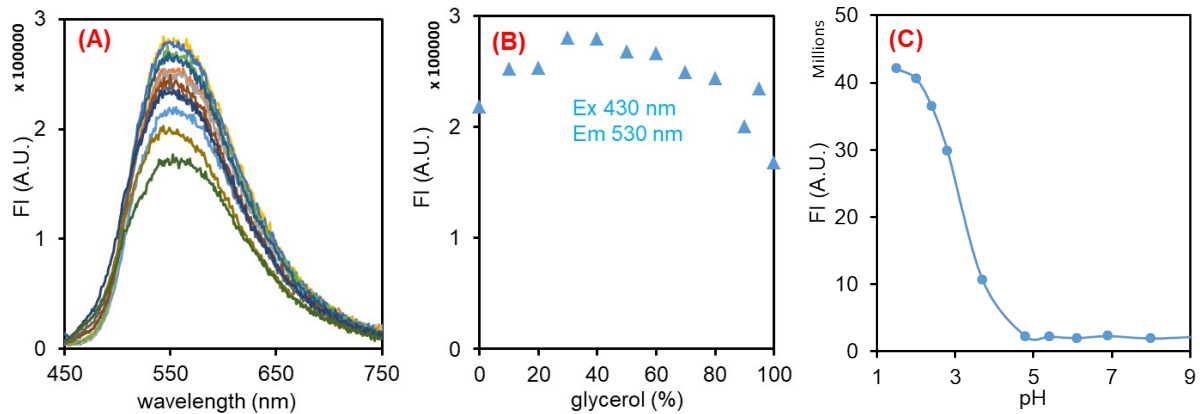


Figure S9: (A) The fluorescence spectra of **BTNN** in water – glycerol binary mixtures; (B) plot of fluorescence intensity of **BTNN** against increasing  $f_{glycerol}$ ; (C) Effect of pH on fluorescence intensity of **BTNN** in glycerol – water 1:1 mixture



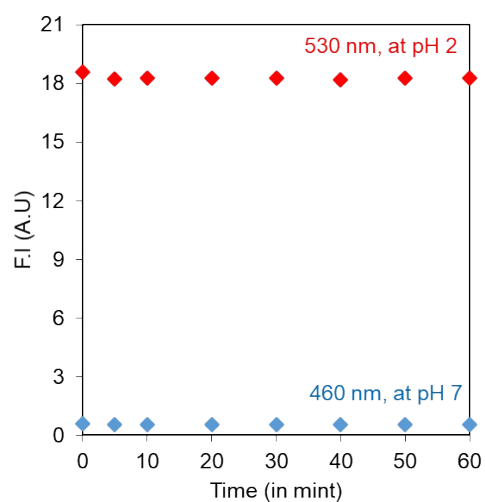


Figure S10: The photo stability of probe **BTNN**

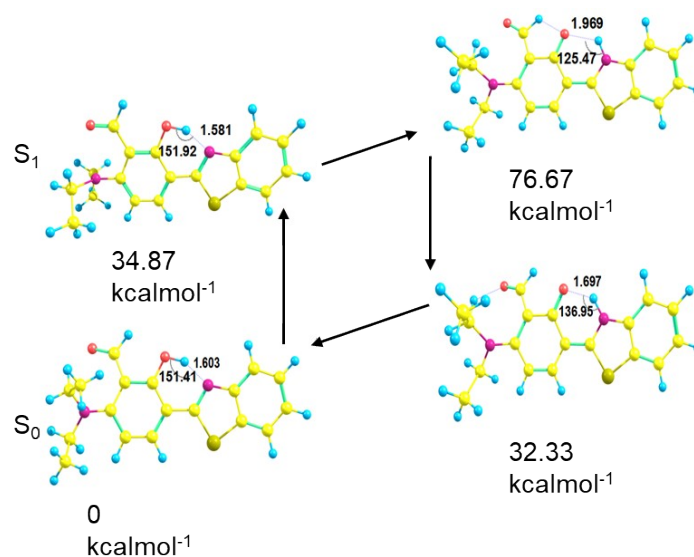


Figure S11: The optimized geometries of normal and keto forms of **BTNN**

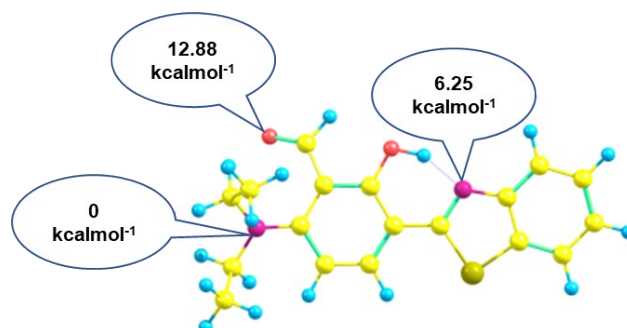


Figure S12: The comparison of relative energies of the **BTNN** obtained after protonation at diethylamino nitrogen, benzothiazole nitrogen and aldehyde oxygen

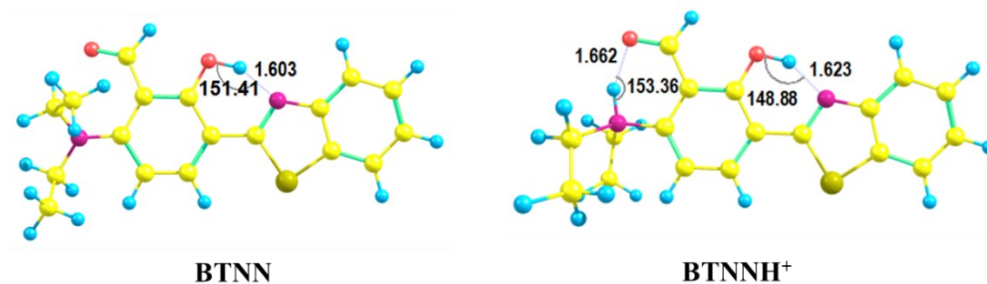


Figure S13: The optimized structures of **BTNN** and **BTNNH<sup>+</sup>**

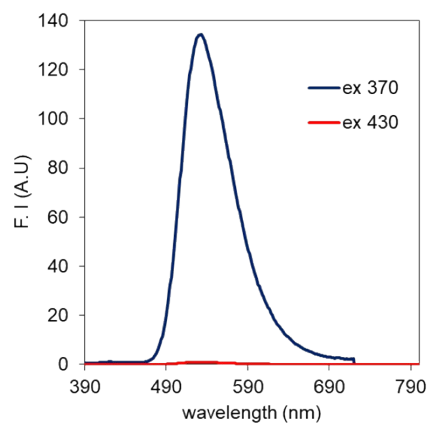


Figure S14: Fluorescence spectra of **BTNN** at pH 2 on excitation at 370 nm and at 430 nm

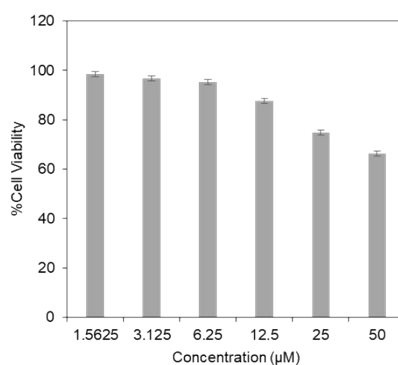


Figure S15: The MTT experiments of **BTNN** under different concentrations for MG-63 cells;

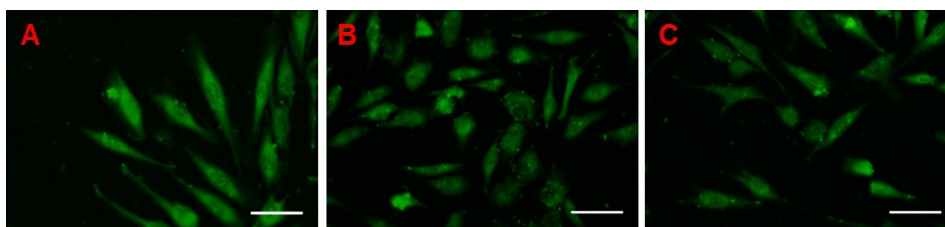
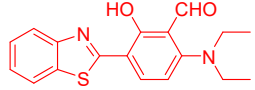
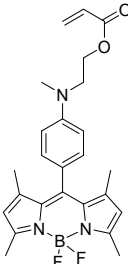
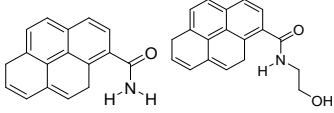

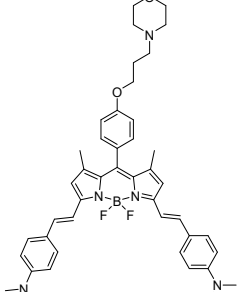
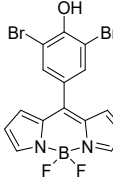
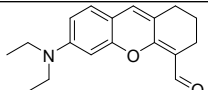
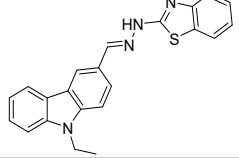
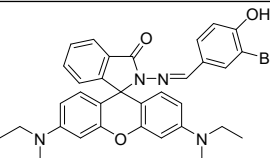
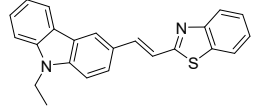
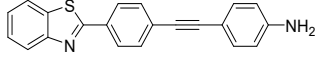
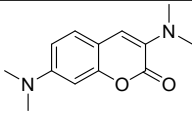
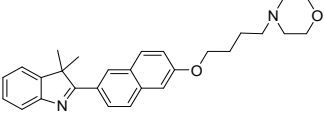
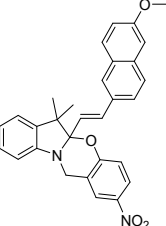
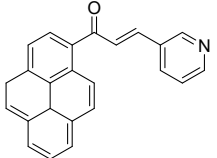


Figure S16: Fluorescence images of the MG-63 cells stained with 10 μM **BTNN** at (A) pH 2.6 (B) pH 3.6 (C) pH 4.6.

**Table S1.** Comparison of physical behaviour and applications of **BTNN** with reported fluorescent probes

S.no	Structure	pk <sub>a</sub>	pH range	Quantum yield	Sensitivity	Live cell imaging	<i>E. coli</i> imaging	Vapour detection	Ref.
1		3.58	2-5	0.69 (at pH 2.0)	146-fold	YES	YES	YES	This work
2		3.48	1.5-4.0	0.017	4.6-fold	YES	YES	YES	1
2		1.93/1.85	1.0-2.5	0.92 / 0.68 (at pH 1)	< 20* (ratio)	NO	NO	NO	2
4		3.00	2.6-4.0	0.65	< 45*	NO	NO	NO	3
5		3.3	1.0-3.0	0.05 (THF)	300 (ratio)	YES	NO	NO	4
6		4.12	3.0-5.0	0.02 (pH 0.5)	750*	NO	YES	NO	5
7		3.11	2.0-4.0	0.60	< 14*	YES	YES	NO	6
8		2.73	2.21-3.30	ND	< 1.4*	NO	YES	NO	7
9		ND	1.75-4.00	ND	< 8*	NO	YES	NO	8

10		1.62	1.23-2.10	0.16 (at pH 1.0)	18 ratio	NO	YES	NO	9
11		1.34	0.5-2.5	0.12 (at pH 0.5)	< 17*	NO	NO	NO	10
12		4.3	3.0-5.0	0.02 (at pH 1.81)	12	vacuolar lumen	NO	NO	11
13		3.65	2.5-4.5	0.35	200*	YES	NO	NO	12
14		3.49	1.8-5.8	0.09 (at pH 2.0)	< 24* ratio	YES	YES	NO	13
15		4.18	2.09-5.0	ND	58 ratio	NO	YES	NO	14

\*calculated from graph

## References

- U. Haldara, S. S. Chaudhury, R. Sharma, B. Ruidas, S. G. Patra, C. D. Mukhopadhyay, H. Lee, *Sens. Actuators B Chem.*, 2020, **320**, 128379.
- T. Liu, Z. Huang, R. Feng, Z. Ou, S. Wang, L. Yang, L. J. Ma, *Dyes Pigm.*, 2020, **174**, 108102.
- F. Ye, X. M. Liang, N. Wu, P. Li, Q. Chai, Y. Fu, *Spectrochim. Acta A Mol. Biomol. Spectrosc.*, 2019, **216**, 359-364.
- M. Zhu, P. Xing, Y. Zhou, L. Gong, J. Zhang, D. Qi, Y. Bian, H. Du, J. Jiang, *J. Mater. Chem.*, 2018, **6**, 4422-4426.
- D. Prasanna and C. Arunkumar, *New J. Chem.*, 2018, **42**, 3473-3482.
- Z. X. Tong, W. Liu, H. Huang, H. Z. Chen, X. J. Liu, Y. Q. Kuang, J. H. Jiang, *Analyst*, 2017, **142**, 3906-3912.
- J. B. Chao, H. J. Wang, Y. B. Zhang, Z. Q. Li, Y. H. Liu, F. J. Huo, C. X. Yin, Y. W. Shi, J. J. Wang, *Anal. Chimica Acta.*, 2017, **975**, 52-60.
- Q. Yang, J. Zou, S. Chirumarry, C. Huo, L. Tang, F. Zhang, X. Peng, *Bull. Korean Chem. Soc.*, 2016, **37**, 1453-1457.
- J. Chao, Y. Liu, J. Sun, L. Fan, Y. Zhang, H. Tong, Z. Li, *Sens. Actuators B Chem.* 2015, **221**, 427-433.
- Y. Tan, J. Yu, J. Gao, Y. Cui, Z. Wang, Y. Yang, G. Qian, *RSC Adv.*, 2013, **3**, 4872-4875.
- J. Joniak, H. Stankovičová, J. Filo, K. Gaplovská-Kyselá, V. Garaj, M. Cigáň, *Sens. Actuators B Chem.*, 2020, **307**, 127646.
- C. B. Martin, J. A. Guadix, J. R. Pearson, F. Najera, J. M. Perez-Pomares, E. Perez-Inestrosa, *ACS sensors.*, 2020, **5**, 1068-1074.

13. J. Peng, H. Chen, M. Sun, H. Yu, J. Hou, S. Wang, *Sens. Actuators B Chem.*, 2021, **335**, 129711.
14. J. B. Chao, Y. X. Duan, Y. B. Zhang, C. X. Yin, M. G. Zhao, J. Y. Sun, F. J. Huo, *Chem Papers*, 2019, **73**, 1481–1488.